

AN IMPROVED RAYLEIGH NUMBER CRITERION FOR FRECKLE PREDICTION INCORPORATING THE EFFECT OF CARBIDES

Y.M. Youssef¹, D. Ness¹, E. Cutler², G.E. Fuchs² and P.D. Lee^{1*}

¹Department of Materials, Imperial College London;
Prince Consort Road, London SW7 2AZ, UK

²Department of Materials Science & Engineering, University of Florida;
P.O. Box 116400, 116 Rhines Hall, Gainesville, FL 32611-6400, USA

*corresponding author: p.d.lee@imperial.ac.uk; +44 207 594 6801

Keywords: Rayleigh number, Freckles, Ni-base superalloys, Carbides.

Abstract

Freckle chains are lines of equiaxed grains which may form during the directional solidification of single crystal Ni-base superalloys. In single crystal alloys freckles form as a result of convective flow of the lighter interdendritic liquid that tends to flow upward towards the heavier bulk composition liquid. Both the interdendritic liquid density and the permeability of the mushy zone affect freckle formation. The Rayleigh number, which is the ratio of the buoyancy to the drag forces in the liquid, is used to assess the likelihood of freckle occurrence. The addition of carbon has been shown to significantly reduce the number of solidification defects, including freckles. The formation of carbides in the interdendritic region will influence both the effective density of the fluid and the structure's permeability. Using a combination of mesoscale solidification modeling and thermodynamic calculations, these two effects were incorporated into an improved Rayleigh number criterion and compared to experimentally observed freckles as a function of the carbon content.

Introduction

The formation of defects during the directional solidification of single crystal Ni-base superalloys can have a significant impact on fatigue and creep properties of some critical components such as turbine blades and discs for aeroengines. Freckles are chains of equiaxed grains preferentially appearing at the component's surface. The formation of freckles has been attributed to the thermal solutal convection in the mushy zone. The evolution of convection currents in the semi-solid (mushy) layer is influenced by the component geometry, the alloy chemical composition and the primary processing parameters such as the thermal gradient and the solidification velocity [1]. The channels resulting from thermosolutal convection in the mushy zone are associated with a variation in density originating from interdendritic segregation. Lighter elements tend to segregate into the interdendritic liquid making it less dense than the bulk liquid. This leads to density-driven flow in the interdendritic region which was proved to initiate freckles.

A widely accepted criterion for the assessment of the alloy's freckling propensity is the calculation of a mushy zone Rayleigh number. The main advantages of using the Rayleigh number are that it combines the effects of alloy composition and processing parameters. However, it does not take into account the component's geometry.

A typical expression describing the Rayleigh number is given by [2]:

$$Ra_h = \frac{gKh}{\alpha\nu} \left(\frac{\Delta\rho}{\rho_0} \right), \quad (1)$$

where ρ_0 is the density of the bulk liquid, g is the gravitational acceleration, ν is the kinematic viscosity, α is the thermal diffusivity, h is the height and K is the permeability of the mushy zone. The term $\Delta\rho/\rho_0$ is the density inversion in the mushy zone and is defined as [3]:

$$\frac{\Delta\rho}{\rho_0} = \left(\frac{\rho_0 - \rho_{(h)}}{\rho_0} \right), \text{ and} \quad (2)$$

$$\rho = \rho_0 \left[1 + \beta_T (T_E - T_0) + \sum_{j=1}^N \beta_C^j (C_E^j - C_0^j) \right], \quad (3)$$

where β_T is the thermal expansion coefficient, β_C^j is the solutal expansion coefficient of element j , N is the number of elements in the alloy, T_E is the eutectic temperature, T_0 is the liquidus temperature, C_E^j is the eutectic composition, C_0^j is the initial composition and ρ_0 is the reference density (the density of the bulk liquid) of the alloy at T_0 and C_0^j .

The uncertainties involved in the calculation of the Ra number lie in the accurate estimation of the different terms, namely the density (as the density inversion effect), the permeability and the viscosity of the interdendritic liquid. The variation of the composition due to the segregation effect of different elements during solidification will have a significant impact on these properties, especially density. The liquid situated in the lower region of the mushy zone consists of light elements such as Al and Ti and is much less dense than the liquid above the mushy zone where no solid has formed. Plumes that rise between the dendrite arms in the liquid have therefore a tendency to form. Hence, concentration-driven convection is expected to happen and is a direct result of elemental segregation.

The addition of small percentages of carbon to superalloys has been proven to reduce the extent of defect formation during solidification. The effect of adding carbon on the formation of carbides has been studied by Tin and Pollock [4-6], Al-Jarba and Fuchs [7] and others [8-10]. Tin and Pollock [4-6] suggested that the addition of carbon reduces the extent of segregation of refractory elements such as Ta, W and Re. This in turn decreases the driving force for thermosolutal convection in the mushy zone. On the other hand, Al-Jarba and Fuchs [7] suggested that the addition of carbon and the consequent presence of carbides in the mushy zone prevent the thermosolutal fluid flow in the interdendritic region. This will have a significant effect on reducing the possibility for freckle formation. It is suggested that the early formation of carbides, at low fraction solid levels, helps in reducing solidification defects since it mitigates the extent of fluid flow and convection in the interdendritic liquid.

It is the objective of the current investigation to study the effect of adding carbon and the presence of carbides on the calculated mushy zone Rayleigh number.

Improved Rayleigh Number Predictions

In order to improve the predictability of the Rayleigh number for freckling formation, a more accurate estimation of the density, permeability and viscosity of the interdendritic liquid is required. The approach used in the estimation of the different properties included in the Rayleigh number calculation is detailed below.

Density estimation

The density of the interdendritic liquid was estimated using the procedure developed by Mills et al., the details of which can be found elsewhere [11]. The general formula for estimating the density ρ_T at any temperature T (where $T \geq$ liquidus temperature) is as follows:

$$\rho_T = \rho_T^{ideal} + \delta\rho_{liq}, \quad (4)$$

where ρ_T^{ideal} is the ideal density of the liquid estimated from the molar volume at temperature T and $\delta\rho_{liq}$ is the change in density to account for the presence of aluminium in the alloy (related to the γ' content and estimated to be = 69.8 x [wt% Al]).

Permeability estimation

Numerically determined microstructures in 3D were obtained using an in-house Cellular Automaton Finite Difference (CAFD) model, combining a cellular automaton growth rule with a finite difference solution of the solute diffusion. Details of the model can be found elsewhere [12-14]. The obtained microstructures were then used in a Computational Fluid Dynamics (CFD) model [15], that numerically solves the Stokes equations and calculates the permeability tensor. Permeability values obtained using 3D slices taken at various locations in the mushy zone were then correlated to the microstructural features, such as primary dendrite arm spacing and fraction solid, using multiple linear regression. The effect of adding carbon was considered by simulating microstructure formation in the presence of carbides. Carbides were assumed to be of MC type (typically TaC; density = $12.8 \times 10^3 \text{ kgm}^{-3}$) and having a blocky shape with an equivalent diameter of approximately 15 μm . The correlation for permeability as a function of different parameters is given by equation 5.

$$\ln(K_{zz}) = b_0 + b_1 \cdot f_s + b_2 \cdot V_f + b_3 \cdot \lambda_1 + b_4 \cdot V_f \cdot f_s, \quad R^2 = 0.98 \quad (5)$$

where K_{zz} is the permeability in the direction parallel to primary dendrite arms, λ_1 is the primary dendrite arm spacing, f_s is the fraction solid and V_f is the volume fraction of carbides. The values of the different coefficients used in the calculation of the permeability using equation 5 are given in Table 1.

Table 1. Coefficients used in the calculation of the permeability in equation 5.

Coefficient				
b_0	b_1	b_2	b_3	b_4
-18.32	-15.76	-1.065	1553.1	2.329

Viscosity estimation

The equation used for estimating the viscosity of liquid superalloys is the one recommended by Mills et al. [11] which is given by the following:

$$\log_{10} \eta_T = 2570/T - 0.8224 + 1.75 \times 10^{-3} X_{Cr} + 1.1 \times 10^{-3} X_{Fe} + 10.2 \times 10^{-3} X_{heavy}, \quad (6)$$

where X_i is the wt% of the element i and X_{heavy} is the sum of the concentrations (wt%) of heavy elements in the alloy (i.e. $X_{heavy} = X_W + X_{Re} + X_{Nb} + X_{Ta} + X_{Mo} + X_{Hf}$).

To account for the presence of carbides in the liquid, an effective (apparent) viscosity, η_T^{eff} , was calculated using the following equation [16]:

$$\eta_T^{eff} = \eta_T (1 + 2.5V_f + 10.05V_f^2), \quad (7)$$

where η_T is the viscosity of the liquid and V_f is the volume fraction of carbides.

Estimation of liquid composition, liquidus temperature and mushy zone height

To account for the variation in the liquid composition as a function of the fraction solid, compositional measurements from Energy Dispersive X-ray Spectroscopy (EDS) analysis on as-cast CMSX4 with a nominal composition as given in Table 2 were used.

Table 2. Nominal composition of CMSX4 alloy investigated.

Composition (wt%)									
Al	Ti	Co	Cr	W	Ta	Re	Mo	Hf	Ni
5.6	1.0	10.0	6.5	6.4	6.5	3.0	0.6	0.1	Bal

The concentrations of the interdendritic liquid at different solid fractions were deduced from the solid compositions using equation 8 [17].

$$C_l = \frac{1}{1 - f_s} \left(C_0 - \int_0^{f_s} C_s df_s \right), \quad (8)$$

where C_0 is the average bulk composition of the solute and C_l is the composition of the interdendritic liquid at the fraction solid f_s . The liquidus temperature, T_l , corresponding to the composition in the interdendritic liquid was calculated using equation 9 [11].

$$T_l \text{ (K)} = 956.9 + 8.2*Y_{Ni} + 7.6*Y_{Co} + 2.2*Y_{Al} + 3.4*Y_{Ti} - 3.7*Y_{Ta} + 3.9*Y_{Cr} + 7.2*Y_{Mo} + 11.5*Y_W + 21.1*Y_{Re} + 12.1*Y_{Ru} + 7.4*Y_{Fe} - 3.3*(Y_{Nb} + Y_{Hf}), \quad (9)$$

where Y_i is the concentration of element i (mole%). The height of the mushy zone, h , was related to the liquidus temperature, T_l , and thermal gradient in the liquid, G_l , as follows:

$$h = \frac{(T_l - T)}{G_l}, \quad (10)$$

where a thermal gradient G_l of 1200 K/m was adopted in the present calculation, which is a typical value for industrial practice.

Results and Discussion

Simulation results showing the 3D dendritic structure are given in Fig. 1a. Fig. 1b shows the flow lines obtained from the CFD simulation around a single blocky carbide particle located next to the dendrite tips.

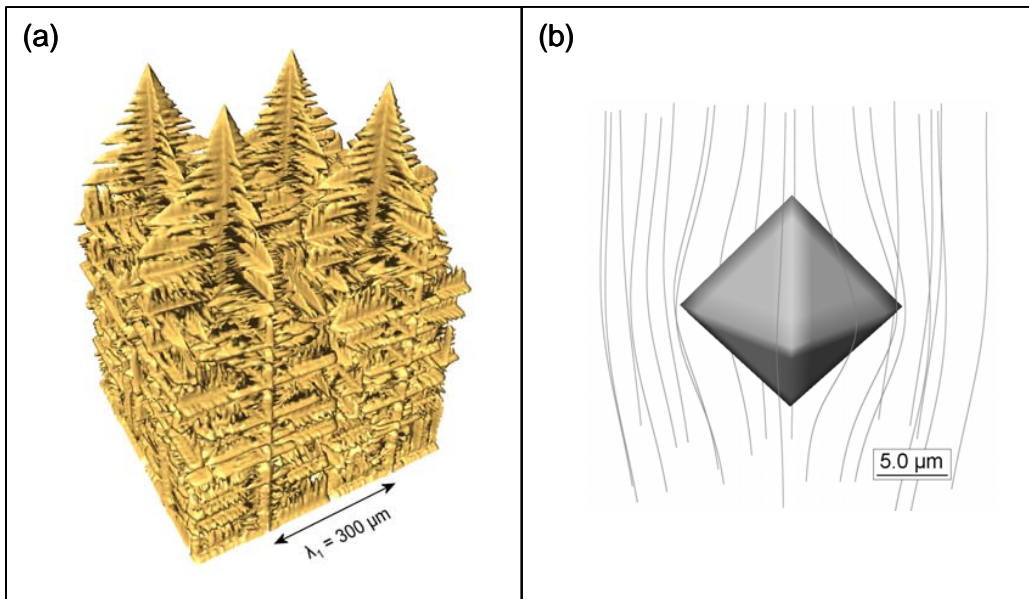


Fig. 1 3D simulation results showing (a) the dendrite structure and (b) the flow lines around a blocky carbide particle within the interdendritic region.

A typical result showing the variation of the mushy zone permeability as function of the fraction solid is given in Fig. 2. The numerical simulations results shown in Fig. 2 agree reasonably well with the predictions from the analytic Blake-Kozeny expression and the expressions suggested by Poirier et al., merged data, [18-20].

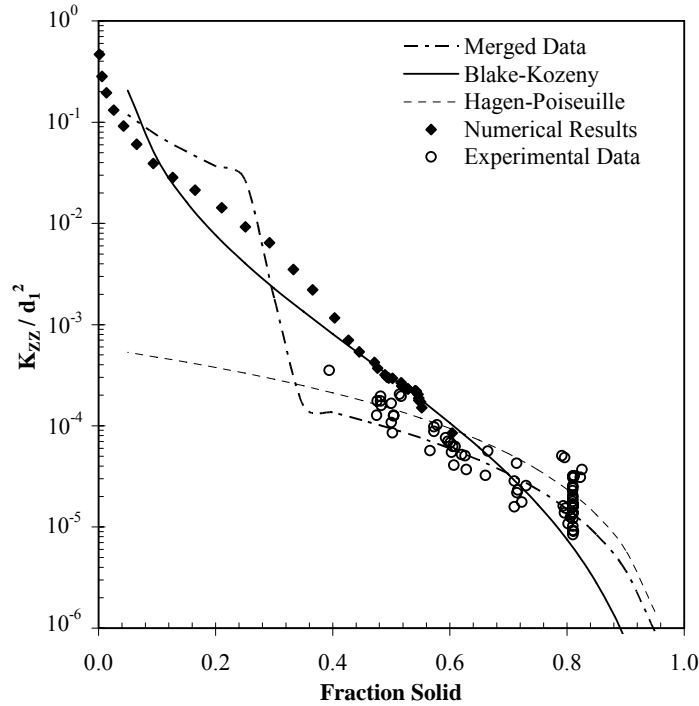


Fig. 2 Variation of permeability with fraction solid calculated numerically and compared to the Poirier (Merged Data), the Blake-Kozeny, the Hagen-Poiseuille and experimental data for Pb-Sn and Borneol-paraffin alloys [18].

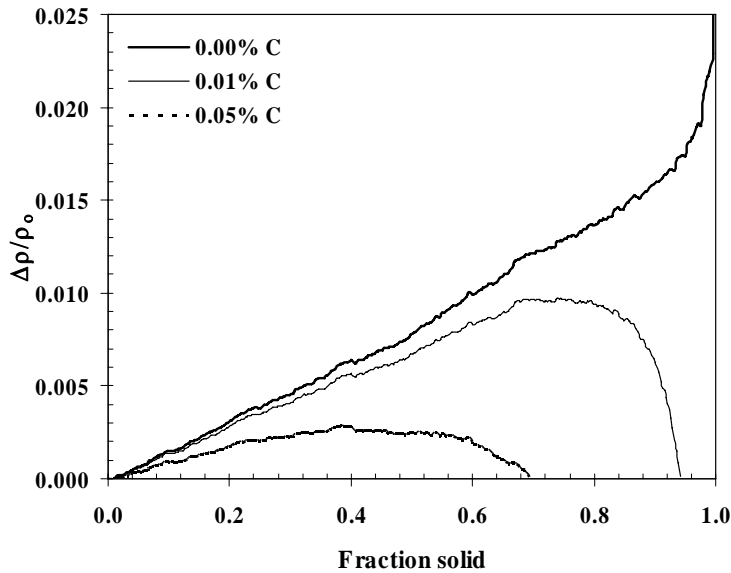


Fig. 3 Effect of carbon addition on the density inversion variation with fraction solid.

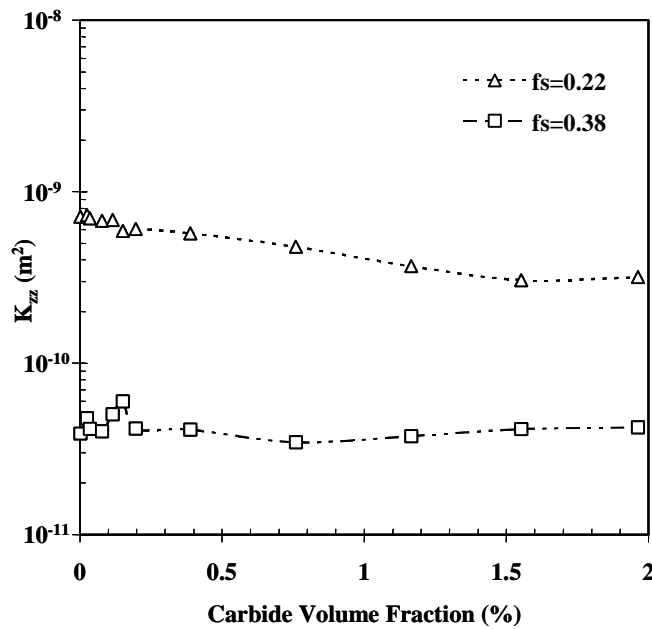


Fig. 4 Effect of carbide volume fraction on the average permeability in the mushy zone for two different fraction solids.

The effect of adding carbon on the extent of density inversion in the mushy zone can be clearly seen in Fig. 3. At 0.3 fraction solid the addition of 0.05 wt% C (~ 0.5 vol% carbides) leads to a reduction of approximately 50% in the extent of the density inversion. Similarly, the effect of carbides on permeability is illustrated in Fig. 4. It can be seen that the addition of 2 vol% carbides results in a reduction of approximately 50% in the mushy zone permeability (K_{zz}).

The predicted mushy zone Rayleigh number as a function of fraction solid for different carbon contents (carbide volume fractions) is shown in Fig. 5. It can be seen from Fig. 5 that the addition of carbon leads to a remarkable reduction in the Rayleigh number especially in the region of approximately 0.2 to 0.3 solid fraction. The region of the mushy zone corresponding to these f_s is believed to be the location where the initiation of freckles takes place. The decrease in the Rayleigh number when carbides are present suggests a significant suppression of thermosolutal convection effects in the mushy zone. The reason for the decrease in the Rayleigh number can be attributed to the effect of carbides on reducing the density inversion effect and permeability. This strongly suggests that both effects have significant impact on the reduction of thermosolutal convection in the mushy zone during solidification. This agrees well with experimental observations that freckle formation is reduced by adding carbon to superalloys [5,7]. The effect of adding carbon on reducing the extent of segregation and the effect on Rayleigh number predictions was not accounted for in the present calculation as suggested by Tin and Pollock. This needs further study and will be an extension to the present investigation.

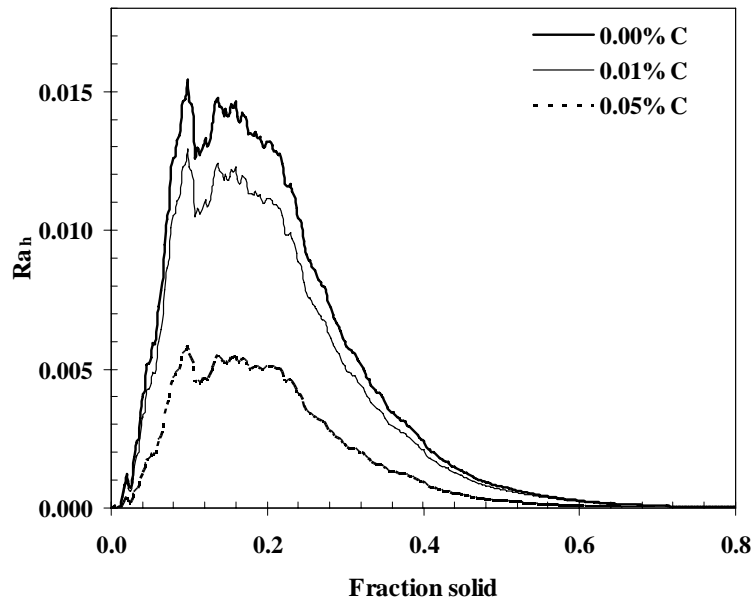


Fig. 5 Effect of carbon addition on the variation of mushy zone Rayleigh number with fraction solid.

Conclusions

The predictability of the Rayleigh number was improved by taking into account the effect of carbides on the reduction in the density inversion, the permeability of the mushy zone and the effect on interdendritic liquid viscosity. The calculated Rayleigh number shows clear evidence that carbides present in the interdendritic region have a significant effect on reducing the extent of density inversion and permeability and hence the possibility for freckle formation. This confirms experimental observations which showed reduced freckles when adding carbon into superalloys.

Acknowledgments

This work was funded by the EPSRC (GR/S45768 & GR/T26344).

References

- [1] Auburtin P, Wang T, Cockcroft SL, Mitchell A. Freckle formation and freckle criterion in superalloy castings. *Metall. Mater. Trans.* 2000;B31:801.
- [2] Beckermann C, Gu JP, Boettinger WJ. Development of a freckle predictor via Rayleigh number method for single-crystal nickel-base superalloy castings. *Metall. Mater. Trans.* 2000;A31:2545.
- [3] Felicelli SD, Poirier DR, Heinrich JC. Macrosegregation patterns in multicomponent Ni-base alloys. *J. Cryst. Growth* 1997;177:145.
- [4] Tin S, Pollock TM, Murphy W. Stabilization of thermosolutal convective instabilities in Ni-based single-crystal superalloys: Carbon additions and freckle formation. *Metall. Mater. Trans.* 2001;A32:1743.
- [5] Tin S, Pollock TM. Stabilization of Thermosolutal Convective Instabilities in Ni-Based Single-Crystal Superalloys: Carbide Precipitation and Rayleigh Numbers. *Metall. Mater. Trans.* 2003;A34:1953.
- [6] Tin S, Pollock TM. Phase instabilities and carbon additions in single-crystal nickel-base superalloys. *Mater. Sci. Eng.* 2003;A348:111.

- [7] Al-Jarba KA, Fuchs GE. Effect of carbon additions on the as-cast microstructure and defect formation of a single crystal Ni-based superalloy. *Mater. Sci. Eng.* 2004;A373:255.
- [8] Chen Q. Effect of alloying chemistry on MC carbide morphology in modified RR2072 and RR2086 SX superalloys. *Scripta Mater.* 2002;47:669.
- [9] Kolotukhin EV, Tjagunov GV. Crystallization of superalloys with various contents of carbon. *J. Mater. Process. Technol.* 1995;53:219.
- [10] Liu LR, Jin T, Zhao NR, Wang ZH, Sun XF, Guan HR, Hu ZQ. Effect of carbon additions on the microstructure in a Ni-base single crystal superalloy. *Mater. Lett.* 2004;58:2290.
- [11] Mills KC, Youssef YM, Li Z, Su Y. Calculation of thermophysical properties of Ni-based superalloys. *ISIJ Int.* 2006;46:623.
- [12] Atwood RC, Lee PD. Simulation of the three-dimensional morphology of solidification porosity in an aluminium-silicon alloy. *Acta Mater.* 2003;51:5447.
- [13] Wang W, Lee PD, McLean M. A model of solidification microstructures in nickel-based superalloys: predicting primary dendrite spacing selection. *Acta Mater.* 2003;51:2971.
- [14] Wang W, Kermanpur A, Lee PD, McLean M. Simulation of dendritic growth in the platform region of single crystal superalloy turbine blades. *J. Mater. Sci.* 2003;38:4385.
- [15] Bernard D, Nielsen O, Salvo L, Cloetens P. Permeability assessment by 3D interdendritic flow simulations on microtomography mappings of Al-Cu alloys. *Mater. Sci. Eng.* 2005;A392:112.
- [16] Lloyd DJ. Particle reinforced aluminium and magnesium matrix composites. *Int. Mater. Rev.* 1994;39:1.
- [17] Yang W, Chen W, Chang K-M, Mannan S, deBarbadillo J. Monte Carlo sampling for microsegregation measurements in cast structures. *Metall. Mater. Trans.* 2000;A31:2569.
- [18] Poirier DR. Permeability for flow of interdendritic liquid in columnar-dendritic alloys. *Metall. Trans.* 1987;B18:245.
- [19] Sung PK, Poirier DR, Felicelli SD. Simulating the initiation of a channel during directional solidification of a superalloy. *Metall. Mater. Trans.* 2001;A32:202.
- [20] Frueh C, Poirier DR, Felicelli SD. Predicting freckle-defects in directionally solidified Pb-Sn alloys. *Mater. Sci. Eng.* 2002;A328:245.